Journal of Nuclear Medicine, published on November 12, 2021 as doi:10.2967/jnumed.121.262958

Anti-Androgen Therapy Radiosensitizes Androgen Receptor Positive Cancers to F-18 Fluorodeoxyglucose

Indulekha Singaravelu,[1] Henry Spitz,[2] Mary Mahoney,[3] Zhongyun Dong,[4]
Nalinikanth Kotagiri *[1]

[1] Division of Pharmaceutical Sciences, James L. Winkle College of Pharmacy, University of Cincinnati, Cincinnati, OH, USA
[23]Department of Nuclear & Mechanical Engineering, University of Cincinnati, Cincinnati, OH, USA
[3]Department of Radiology, University of Cincinnati College of Medicine, Cincinnati, OH, USA
[4]Division of Hematology & Oncology, University of Cincinnati College of Medicine, Cincinnati, OH, USA
*Corresponding author. E-mail: kotaginh@ucmail.uc.edu

Funding (N.K):
CDMRP BRCA Breakthrough Award: W81XWH-18-1-0609
NIH: U54 CA199092
University of Cincinnati Strategic Collaborative Grant

Corresponding author contact information:
Nalinikanth Kotagiri
231 Albert Sabin Way, MSB 3005K
Cincinnati, OH 45267
Phone: 513-558-6161
Fax: 513-558-3095
Email: kotaginh@ucmail.uc.edu

First author contact information:
Indulekha Singaravelu
Phone: 513-628-7445
Email: indulekhas@outlook.com

Running title:

Combination hormonal ^{18}F-FDG therapy

ABSTRACT

Background: A subset (35%) of triple negative breast cancers (TNBC) express androgen receptor (AR) activity. However, clinical trials with anti-androgen drugs have shown limited efficacy with about a 19% clinical benefit rate. We investigate the therapeutic enhancement of anti-androgens as radiosensitizers in combination with ^{18}F-fluoro-2-deoxy-D-glucose (^{18}F-FDG) in TNBC.

Methods: We screened five candidate drugs to evaluate shared toxicity when combined with either ^{18}F-FDG, X-ray or ultraviolet (UV) radiation, at doses below their respective sub-IC_{50} values. Cytotoxic enhancement of anti-androgen in combination with ^{18}F-FDG was evaluated using cell proliferation and DNA damage assays. Finally, therapeutic efficacy of the combination treatment was evaluated in mouse tumor models of TNBC and prostate cancer.

Results: Bicalutamide (Bical), an anti-androgen drug, was identified to share similar toxicity in combination with either ^{18}F-FDG or X-rays, indicating its sensitivity as a radiosensitizer to ^{18}F-FDG. Cell proliferation assays demonstrated selective toxicity of combination Bical-^{18}F-FDG in AR-positive 22RV1 and MDA-MB-231 cells in comparison to AR-negative PC3 cells. Quantitative DNA damage and cell cycle arrest assays further confirmed radiation induced damage to cells suggesting the role of Bical as a radiosensitizer to ^{18}F-FDG-mediated radiation damage. Animal studies in MDA-MB-231, 22RV1 and PC3 mouse tumor models demonstrated significant attenuation of tumor growth through combination of Bical and ^{18}F-FDG in the AR-positive model in comparison to the AR-negative model. Histopathology corroborated the *in vitro* and *in vivo* data and confirmed the absence of off-target toxicity to vital organs.

Conclusions: These data provide evidence that ^{18}F-FDG in conjunction with anti-androgens serving as radiosensitizers has utility as a radiotherapeutic agent in the ablation of AR-positive cancers.

Keywords:
Anti-androgen therapy; bicalutamide; radiosensitization; ^{18}F-FDG

INTRODUCTION

Concomitant chemotherapy and radiation therapy is an established treatment regimen for many neoplasms (*1-3*). For example, paclitaxel (Taxol), besides its antiangiogenic properties, is also known to enhance the therapeutic effects of ionizing radiation as revealed in clinical trials (*4*). Thus, the risks associated with use of both radiotherapy and drug usage are considerably high due to unintentional radiation-drug interactions (*5*). Therefore, there is a need for systematic examination of drug-radiation interactions, and more fundamentally, photochemical and biological interactions between different classes of drugs and radiation in order to enhance therapeutic outcomes.

Recent studies show that radionuclides, in contrast to external beam radiation, can provide the flexibility and extended reach *in vivo* to trigger therapeutic events in niches where metastatic cancer cells tend to localize, such as bone marrow and lungs (*6,7*). Typically, emissions from radionuclides include: (1) Ionizing radiation, comprised of either electron (β^-), positron (β^+), alpha (α) particles, Auger electrons, x-ray and gamma (γ) photons; (2) Non-ionizing radiation, comprised of luminescence and ultraviolet (UV)-blue light emitted by beta (β) particles, known as Cherenkov radiation. The various types of emissions from a single radionuclide can drive new opportunities in determining beneficial effects in combination with drugs. Due to the associated complexity in dosimetry it can also be challenging as these combinations can lead to unintended consequences if the treatment strategy is not optimized. For example, a recent phase III trial of vaginal cuff brachytherapy in combination with paclitaxel/carboplatin chemotherapy in patients with high-risk, early stage endometrial cancer resulted in acute toxicities to the patients (*8*). Therefore, in our study we sought to identify and characterize compounds that are capable of efficiently harvesting the different energy emissions

from diagnostic radionuclides to trigger therapeutic outcomes through synergistic action, without causing radiation or drug toxicity.

Since ^{18}F-fluoro-2-deoxy-D-glucose positron emission tomography (^{18}F-FDG-PET) scans are routinely used in the evaluation of breast cancer patients, we postulated that by leveraging this technique for activating light sensitive FDA approved drugs, we could potentially transform toxic chemotherapeutics to nontoxic targeted therapy of untargetable cancers, such as Triple Negative Breast Cancer (TNBC). In this study, we screened various anticancer drugs and explored synergy with different types of radiation sources to identify drugs that exhibit significantly higher toxicity against cancer cells when used in combination with ^{18}F-FDG. Previous studies have explored how non-ionizing radiation from radionuclides can be harnessed by drugs and nanoparticles for photoactivated therapy (*6*,*9*). In this study we explore how ionizing radiation from diagnostic radionuclides can be used in combination with certain drugs for enhanced cancer therapy while minimizing off-target effects.

MATERIALS & METHODS

Drug Screening in Combination with ^{18}F-FDG

All drugs (Bicalutamide, flutamide, Dacarbazine, 5-fluorouracil and titanocene) were purchased from Apexbio Inc. Drugs were resuspended in DMSO and aliquots prepared. In vitro efficacy of the drugs was investigated in MDAMB231 cell line (ATCC). Cells were treated with drugs at sub-toxic dosage which was followed by addition of three different activities (7.4, 14.8, 29.6 MBq) of the radiopharmaceutical, ^{18}F-FDG, procured in PBS. Media was replaced after one half-life of ^{18}F, approximately 110 min of incubation to remove excess ^{18}F-FDG that did not internalize in cells. Cell viability was evaluated after 72 hours by measuring the mitochondrial

activity in live cells using MTS reagent (Promega Cell proliferation reagent) and absorbance measurement at 490 nm by Cytation I (BioTek instruments) in triplicate. Similarly, cell viability was also measured for the cells pre-treated with drugs with UV light [UVP mini UV lamp, 4 watt, 365 nm & 254 nm] for one hour and ionizing radiation [x-ray irradiator, Xen-X Irradiator, 50-220 kV x-rays]. An exposure of 2 Gy was used, which is a clinically used exposure limit for therapeutic purpose. The assays were repeated three times.

AR Expression on Cancer Cells and Cytotoxicity Assessment

AR expression of 22RV1, PC3, MDAMB231 and MCF10A cells (ATCC) was measured by flow cytometry. Cells were stained using standard procedures as outlined in the supplementary section. The stained cells were analyzed for androgen receptor (AR) expression in flow cytometry (BD / LSRII). The assays were repeated three times for each cell line. Toxicity of Bicalutamide (Bical) combined with ^{18}F-FDG treatment was evaluated using MTS assays in the cell lines following manufacturers instructions.

DNA Damage Assessment

DNA damage caused by Bical-^{18}F-FDG in MDAMB231 was determined by cell death detection assays and γH2AX phosphorylation assays. A dose of 7.4 MBq of ^{18}F-FDG was henceforth used for all *in vitro* and *in vivo* experiments. Additional details of cell death detection assay is outlined in the supplementary section.

To measure γH2AX phosphorylation of histones, cells were harvested in the 96-well plate with the seeding density of 10^4 per well, treated with Bical-^{18}F-FDG, Bical, ^{18}F-FDG, and

untreated cells in triplicate using an EMD Millipore H2A.X phosphorylation assay kit. Details in supplementary section.

Evaluation of Cell Death Mechanism

Apoptotic cell death and autophagy was quantified by flow cytometry analysis using Annexin V-FITC/PI (propidium iodide) staining and autophagy detection kit (Enzo Life Sciences), respectively. Cell cycle analysis was performed by staining the fixed cells with PI dye. Details in supplementary section.

Efficacy of Combined Bical-^{18}F-FDG Treatment in Animal Models

MDAMB231,22RV1 and PC3 cultured cancer cells (2 x 10^6 cells) admixed with Matrigel were injected subcutaneously in the flank regions of 6-8 week old female and male Athymic nude mice (Jackson laboratory). When the tumor reached 200–250 mm^3, mice were randomized into different treatment groups (n=5 animals per group). Bicalutamide was administered orally every week at a dose of 60 mg/kg bodyweight and 7.4 MBq ^{18}F-FDG was injected via an intraperitoneal route for four weeks. Mice were monitored every two days for a period 30-60 days for survival, adverse effects and weight loss. Treatment efficacy was evaluated in comparison with untreated, Bical alone and ^{18}F-FDG alone as control groups. Additional discussion on small animal ^{18}F-FDG activity is outlined in the supplementary section (*10*).

Statistical Analysis

All experiments were performed in triplicate and statistical analyses were performed using GraphPad Prism 8 software. P values were determined by the one-way analysis of variance

(ANOVA) method and $P < 0.01$ was considered statistically significant in all experiments wherever applicable. Results obtained from in vitro and in vivo analysis were shown as means ± SD or SEM of three or more independent experiments. Statistical values shown in figures were based on values, *P < 0.01, **P < 0.001.

RESULTS

Evaluation of Toxicity of Drugs in Combination with ^{18}F-FDG

We evaluated five anticancer drugs – 5-fluorouracil, dacarbazine, flutamide, bicalutamide (Bical) and titanocene – based on their already established photosensitive properties. 5-fluorouracil (5-FU) is known to induce protein degradation through superoxide radical and photooxidation mechansims upon UV irradiation (*11*). Dacarbazine is a photosensitive drug known to synergize with light to produce increased toxicity through photodegradation mechanism (*12*). Flutamide and Bical are known to be photoreactive and induce photosensitive drug eruptions in patients (*13,14*). Titanocene is a UV sensitive compound that exhibits enhanced phototoxicity through photodegradation mechanism (*6,7*). While all five drugs are known to be light sensitive, it is unclear which type of radiation, ionizing or nonionizing, are the drugs sensitive to. Since ^{18}F-FDG generates both UV and ionizing radiation, we sought to identify specifically which radiation among the two triggered cell death in combination with drugs. Our first objective was to estimate their dark-toxicity by identifying their IC_{50} values in MDAMB231 cells, a representative TNBC cell line (Supplemental Fig. 1). The drugs were then screened and evaluated for inducing cytotoxicity, at doses below their respective sub-IC_{50} values, in combination with either ^{18}F-FDG, X-ray and UV radiation. Based on the estimated IC_{50}

values, a dose of 3.12 μM, 50 μM, 25 μM, 12.5 μM and 25 μM was selected for 5-FU, titanocene, dacarbazine, flutamide and bical, respectively.

All five drugs showed enhanced toxicity when treated with ^{18}F-FDG. However, toxicity profile for the drugs was unique with respect to sensitivity to UV light, radiation or both (Fig. 1A, B). Besides ^{18}F-FDG, 5-fluorouracil and titanocene exhibited cytotoxicity in combination with UV light. Similarly, besides ^{18}F-FDG, flutamide and bical exhibited cytotoxicity exclusively in combination with X-rays. Dacarbazine, however, exhibited cytotoxicity in combination with both UV and X-rays, as well as ^{18}F-FDG. These results suggest that ionizing (flutamide, bical, dacarbazine) and/or nonionizing radiation (5-FU, titanocene, dacarbazine) emitted by the radioactive decay of ^{18}F could be playing a role in triggering these drugs. The lower cytotoxicity of UV treated cultures treated with flutamide and bicalutamide, compared to drug alone likely suggests drug photoinactivation (*15*).

Bicalutamide Radiosensitizes Cancer Cells to ^{18}F-FDG and X-rays

Bical is a molecularly-targeted anti-androgen drug, which also has radiosensitizing properties. Therefore, we hypothesized that Bical in combination with ^{18}F-FDG will likely enhance cytotoxicity and provide greater control in spatiotemporal modulation of this therapeutic approach. First, we investigated the photophysics behind the reactants, Bical and ^{18}F-FDG. Photoproducts formed by photoreaction of the drugs with UV light typically causes type IV hypersensitive (cell-mediated) reactions (*16*). However, we noted earlier that Bical in the presence of UV light did not induce cytotoxicity. To further confirm whether UV irradiation of Bical induces the generation of photoproducts, we performed Mass spectrometry and Fourier-transform infrared spectroscopy analysis. We observed no change in the structure (Supplemental

Fig. 2) and molar mass (Supplemental Fig. 3) of Bical, suggesting the parent compound was stable even after irradiation with UV light. These results suggest that irradiating Bical with ^{18}F-FDG likely results in minimal photodegradation. However, to explain the enhanced toxicity observed with Bical-^{18}F-FDG, it is possible that there is biological cooperation, with Bical blocking the androgen receptor (AR) and inhibiting DNA damage repair, and thereby increasing the susceptibility of cancer cells to radiation damage by ^{18}F-FDG (*17*).

Cytotoxic Enhancement of Bical & ^{18}F-FDG Combination in AR Positive Cancer Cells

We analyzed four human cancer cell lines, two prostate and two breast cancers, for AR expression by flow cytometry. The prostate cancer cell lines were 22RV1 and PC3 and breast cancer cell lines were MDAMB231 and MCF10A, where the latter is a normal breast epithelial cell line. While MCF10A and PC3 cells did not display any significant AR expression (Supplemental Fig. 4A,B), an estimated 85% of the cultured 22RV1 and 81% of MDAMB231 cells expressed AR (Supplemental Fig. 4C,D). We then evaluated the cytotoxicity of Bical-^{18}F-FDG combination on AR positive 22RV1 and MDAMB231 and AR negative MCF10A and PC3 cells. We observed that even at a subcytotoxic dose of 25 μM, cytotoxicity (IC_{20}) of Bical was significantly enhanced after exposure to activity as low as 7.4 MBq in both MDAMB231 and 22RV1 cells, whereas the IC_{20} value of Bical alone was 65 μM (Fig. 2A,B). We observed activity dependent increase in cytotoxicity with 7.4, 14.8, 29.6 MBq ^{18}F-FDG. Both MCF10A and PC3 cells were unresponsive to both Bical alone and Bical-^{18}F-FDG treatment even at a dose of 50 μM (Fig. 2C,D). These results suggest that the combination of Bical-^{18}F-FDG is selectively inhibiting the proliferation of AR positive cells over non-AR expressing cells at subcytotoxic monotherapy doses.

Bical-^{18}F-FDG Treatment causes DNA Damage

We first investigated whether the cells were experiencing oxidative damage to their DNA, which is typical in radiotherapies. Relative quantification of the DNA fragments obtained in the cell lysate post-treatment with Bical and 7.4 MBq ^{18}F-FDG in MDAMB231 cells was correlated with DNA damage, which is generally considered as an early indicator of apoptosis. Using a quantitative ELISA based assay to detect mono- and oligonucleosomes, we observed that Bical-^{18}F-FDG treatment was found to induce increased DNA damage to the cells compared to Bical alone,^{18}F-FDG alone, and untreated groups (Fig. 3A). DNA damage was observed to be higher at 5 hours post treatment compared to 48 hours, mainly since nucleosomes are detected before the cascade of other apoptotic events start manifesting; and also due to the fact that there are likely to be lower number of intact viable cells at the 48 hour timepoint as a consequence of apoptosis.

Phosphorylation of H2AX histone protein typically occurs when DNA double strand breaks are induced during exposure of cancer cells to chemotherapeutics or radiation, resulting in DNA rearrangement or apoptosis. Bical-^{18}F-FDG treatment resulted in a significantly higher chemiluminescence measurement, which is correlated to high amounts of γH2AX protein from increased double strand breaks in the DNA (Fig. 3B).

Cell cycle and DNA content analysis showed no significant increase in cells occupying the G1/S phase 24 hours post treatment. However, 32.8% of the cells were occupying the G2/M phase when treated with Bical-^{18}F-FDG, compared to 18.3% in Bical alone, and 17.3% in ^{18}F-FDG treated, and untreated cells (Fig.3C). This study indicates that the anti-proliferative characteristics of Bical-^{18}F-FDG treatment in cancer cells is from G_2/M cell cycle arrest after

inducing DNA damage, thus preventing the cells with DNA damage from entering the M phase and undergoing mitosis.

Cell Death Mechanism – Apoptosis & Autophagy

Apoptotic cell death is characterized by distinct morphological changes like cell shrinkage, DNA condensation, and cell blebbing. These biochemical processes, involving various signaling pathways, are triggered when cells undergo DNA damage and cell cycle arrest. Bical-^{18}F-FDG (7.4 MBq ^{18}F-FDG, 25 μM Bical) treated MDAMB231 cells were evaluated using flow cytometric analysis of Annexin V-FITC / Propidium iodide (PI) staining. Fig. 4 shows that 32.7% of Bical-^{18}F-FDG treated cells were found to be in the late apoptotic (LA) state, since they stained positive for both Annexin V-FITC and PI. In contrast, only 10.6% of untreated and 18.6% of Bical alone treated cells stained with both Annexin V-FITC and PI. Annexin V- FITC stains cells undergoing apoptosis by staining phosphatidylserine molecules that have translocated to the outside of the cell membrane, while PI stains cells that are necrotic or late apoptotic cells, which are characterized by the loss of the integrity of the plasma and nuclear membranes. The high degree of DNA fragmentation and double staining of cells with Annexin V and PI, suggests apoptosis, rather than necrosis, to be the dominant cell death mechanism as a result of Bical -^{18}F-FDG treatment.

We next examined whether cells were undergoing autophagy, since ionizing radiation has been shown to induce autophagy in cancer cells (*18*). The autophagic process is a regulated mechanism involving swelling of the cell membrane and formation of autophagosomes to degrade and recycle the intracellular contents. Quantification of cell death by the autophagic process was performed by analyzing cells stained with Cyto-ID® green dye using a Flow

cytometer. Cyto-ID® stains AVOs green at different stages in the process of autophagy before it fuses with lysosomes and is internalized. Fig. 5 and Supplemental Fig. 5 clearly shows a higher fluorescence intensity and upregulation of autophagic activity in cells treated with combined Bical-^{18}F-FDG when compared to Bical alone, ^{18}F-FDG treated, and untreated cells. Rapamycin and chloroquine treated cells were used as positive controls.

Efficacy of Combination Bical-^{18}F-FDG Treatment in Mouse Xenograft Models

After initiation of treatment, we started observing significant separation in the tumor volume curve of Bical-^{18}F-FDG treated mice group compared to the rest, as shown in Fig. 6A,B. Overall, combination treatment with Bical and ^{18}F-FDG exhibited significant attenuation in tumor growth compared with that of Bical alone and ^{18}F-FDG alone, which were not statistically different from the untreated group. Histopathological analysis of immunostained MDAMB231 tumor tissues (Supplemental Fig. 6A) revealed Bical-^{18}F-FDG treated tumor tissues stained highly positive for cleaved caspase-3 which is an expression marker for apoptosis and DNA damage. Similarly, with Ki67 staining, which is a marker for highly proliferating cells, there was a significant reduction in the Ki67 staining with Bical-^{18}F-FDG treated tumors. We also observed decreased CD68- stained positive cells, which suggests lower degrees of macrophage infiltration within the tumor. Typically, increased tumor growth is also characterized by the presence of CD68 expressing tumor infiltrating macrophages (TAMs), playing a key role in promoting tumor initiation and malignant progression. In addition, H&E staining of brain, heart, liver and kidney confirmed that there was no evidence of metastatic spread to these organs, as well as any treatment related off-target toxicity (Supplemental Fig. 6B).

To elucidate the role that AR targeted Bical plays in this 'dual-specific' strategy, a similar experiment was performed with an AR negative prostate cancer xenograft model in male nude mice using PC3 cells. Unlike in the AR+ cancer models, the Bical-^{18}F-FDG treated group did not show any significant difference from the ^{18}F-FDG and Bical control arms (Fig. 6C). Interestingly, there was a significant increase in PC3 tumor attenuation in mice treated with ^{18}F-FDG compared to untreated and Bical alone treated mice, further confirming the critical role that AR plays in sensitizing the cells to ^{18}F-FDG in TNBC. Histopathological analyses with TUNEL staining (DNA damage causing cell death) and CD68 staining assay for TAMs did not indicate any degree of tumor ablation at the tissue level, as shown in Supplemental Fig. 6C,D. Due to the non-tumorigenic nature of MCF10A cells, tumor induction was not possible for this model.

DISCUSSION

TNBC is an aggressive cancer that lacks estrogen, progesterone and HER2 receptors and therefore cannot be treated with targeted hormone therapies or anti-HER2 treatments (*19*). As a result, conventional "always on" chemotherapy remains the only effective systemic treatment available for these patients. Recent studies have reported that approximately 35% of TNBC patients have shown expression of membrane AR (*20*). While the role of AR in TNBC is an area of active research, there is evidence that this cancer subset may respond to therapeutic targeting of AR (*21*). Bical functions by blocking and inhibiting AR and is widely used in the treatment of male prostate cancer subtypes that overexpress AR (*22*). However, clinical trials with Bical and other antiandrogen drugs in TNBC have shown limited efficacy with about a 19% clinical benefit rate (*21*). Therefore, we hypothesized that Bical activated cytotoxic enhancement of ^{18}F-FDG would improve therapeutic outcomes of the combination treatment in TNBC and provide

spatiotemporal modulation of therapy as well. This hypothesis is supported on the basis that AR activity has influence on cell cycle checkpoint inhibition and the DNA damage repair pathway (*23*,*24*). Prior research has also demonstrated that anti-androgen drugs that block AR activity confer radiosensitivity to traditionally radioresistant AR-positive, TNBC cell lines by significantly impairing resolution of double stranded (ds) DNA breaks (*17*). Although TNBCs are chemo-sensitive, they are found to metastasize rapidly and are characterized by poor prognosis and few therapeutic options. Therefore, using radionuclides, in contrast to external beam radiation, permits the extended reach *in vivo* to trigger therapeutic events in niches where metastatic cancer cells tend to localize, such as bone marrow and lungs.

It is important to note that while both targeted hormonal therapy and radiosensitizing roles for Bical would be highly desired in a clinical setting, for our proof-of-concept studies we sought the effective separation of both these properties in order to evaluate the singular role of Bical as a radiosensitizer. *In vitro* studies revealed that a subcytotoxic dose of Bical in combination with ^{18}F-FDG inhibited cell proliferation, induced dsDNA breaks and caused cell cycle arrest at the G2/M phase, leading to apoptotic cell death. Therefore, we can infer that Bical is a potent radiosensitizer because it selectively inhibits DNA damage repair of AR positive cells caused by ^{18}F-FDG.

Previous reports have shown that apoptosis only accounts for approximately 20% of radiation-induced cell death (*25*). Therefore, we explored other cell death pathways, such as autophagy, to determine if multiple pathways are involved in inducing cell death. We observed significant cell death through autophagy, implicating the role of endoplasmic reticulum (ER) stress and aberrant protein folding leading to the formation of autophagosomes. While there is still no consensus on attributing specific mechanisms that link radiation and autophagy, there is

some evidence that dsDNA breaks may induce ER stress (*26*). Enhanced therapeutic efficacy of the combination treatment in TNBC cells appears to have significant contribution from both autophagy and apoptosis cell death pathways.

In vivo therapy studies in an AR-positive TNBC and 22RV1 mouse models showed significant attenuation of tumor growth and enhanced therapeutic efficacy in group of mice treated with Bical-^{18}F-FDG compared to control groups that were not statistically different. The therapeutic effect of Bical alone was minimal, which can be attributed to the subtherapeutic concentration used for these studies. However, in an AR-negative PC3 mouse model, we observed no significant attenuation of tumor growth, supporting the critical role Bical plays in radiosensitizing the AR-positive tumors to radiation-induced damage from ^{18}F-FDG. Further studies are needed to elucidate the mechanism of enhanced therapeutic efficacy – synergistic vs. additive – before translation of this strategy could potentially be realized.

With ^{18}F-FDG, we avoided using excessively high or non-diagnostic imaging activity to demonstrate not only the efficiency of Bical as a radiosensitizer in reducing the threshold for radiation damage, but also to allay any concerns regarding potential toxicity during scale-up for translational studies, where higher activities of ^{18}F-FDG might be deemed unrealistic for use in humans (*10*). However, additional studies are needed to understand the dosage expectancy of ^{18}F-FDG for potential clinical translation. Gross morphological analysis as well as H&E analysis of major organs did not reveal any off-target toxicity from treatment. Indeed, further studies are required to estimate absorbed dose in normal organs and collect additional evidence to confirm the absence of off-target toxicity to various vital organs such as brain and bone marrow.

CONCLUSION

We have demonstrated the sensitivity of AR-positive cancer to radiation damage using the diagnostic radiopharmaceutical, ^{18}F-FDG, in conjunction with Bical, an antiandrogen that serves as a targeted radiosensitizer. These findings open opportunities to investigate other antiandrogens and radionuclides, as synergistic pairs, to enhance therapeutic outcomes. Given the wide range of radionuclides available, studies exploring the mixed radiation emissions and interaction with drugs to identify synergistic enhancement of cell killing would be intriguing.

DISCLOSURES

The authors disclose no potential conflicts of interest.

ACKNOWLEDGEMENTS

The authors would like to thank the Radiation safety staff at the University of Cincinnati for assistance with the handling of radioactive materials. The authors also acknowledge the help provided by Shindu Thomas and Tushar Madaan with animal experiments; Sithara Raju Ponny with data analysis; Betsy DiPasquale and Jessica Webster in preparing samples for IHC; Larry Salans with the Mass spectrometry studies; Mallikarjuna Nadagouda with the FTIR studies; and the Flow cytometry core at the Cincinnati children's hospital.

KEY POINTS

Question: We asked the question whether anti-androgen hormonal therapy could radiosensitize androgen receptor positive cancers to ^{18}F-FDG.

Pertinent Findings: Preclinical studies using combination of bicalutamide and ^{18}F-FDG were conducted in both AR positive and AR negative mouse tumor models. We observed a significant attenuation, two-fold, of tumor growth in AR positive compared to AR negative cancers.

Implications for patient care: We envisage that this strategy will benefit AR positive cancer patients with metastatic burden in providing an effective image-guided targeted therapy with minimal side effects.

REFERENCES

1. Apisarnthanarax S, Dhruva N, Ardeshirpour F, et al. Concomitant radiotherapy and chemotherapy for high-risk nonmelanoma skin carcinomas of the head and neck. *Int J Surg Oncol.* 2011;2011:464829.

2. Glatzer M, Elicin O, Ramella S, Nestle U, Putora PM. Radio(chemo)therapy in locally advanced nonsmall cell lung cancer. *Eur Respir Rev.* 2016;25:65-70.

3. Calais G, Alfonsi M, Bardet E, et al. Randomized trial of radiation therapy versus concomitant chemotherapy and radiation therapy for advanced-stage oropharynx carcinoma. *J Natl Cancer Inst.* 1999;91:2081-2086.

4. Dicker AP, Williams TL, Iliakis G, Grant DS. Targeting angiogenic processes by combination low-dose paclitaxel and radiation therapy. *Am J Clin Oncol.* 2003;26:e45-53.

5. Niyazi M, Maihoefer C, Krause M, Rodel C, Budach W, Belka C. Radiotherapy and "new" drugs-new side effects? *Radiat Oncol.* 2011;6:177.

6. Kotagiri N, Sudlow GP, Akers WJ, Achilefu S. Breaking the depth dependency of phototherapy with Cerenkov radiation and low-radiance-responsive nanophotosensitizers. *Nat Nanotechnol.* 2015;10:370-379.

7. Kotagiri N, Cooper ML, Rettig M, et al. Radionuclides transform chemotherapeutics into phototherapeutics for precise treatment of disseminated cancer. *Nature Communications.* 2018;9:275.

8. Randall ME, Filiaci V, McMeekin DS, et al. Phase III Trial: Adjuvant Pelvic Radiation Therapy Versus Vaginal Brachytherapy Plus Paclitaxel/Carboplatin in High-Intermediate and High-Risk Early Stage Endometrial Cancer. *J Clin Oncol.* 2019;37:1810-1818.

9. Pratt EC, Shaffer TM, Zhang Q, Drain CM, Grimm J. Nanoparticles as multimodal photon transducers of ionizing radiation. *Nature Nanotechnology.* 2018;13:418-426.

10. Taylor K, Lemon JA, Boreham DR. Radiation-induced DNA damage and the relative biological effectiveness of 18F-FDG in wild-type mice. *Mutagenesis.* 2014;29:279-287.

11. Miolo G, Marzano C, Gandin V, et al. Photoreactivity of 5-Fluorouracil under UVB Light: Photolysis and Cytotoxicity Studies. *Chemical Research in Toxicology.* 2011;24:1319-1326.

12. Dorr RT, Alberts DS, Einspahr J, Mason-Liddil N, Soble M. Experimental dacarbazine antitumor activity and skin toxicity in relation to light exposure and pharmacologic antidotes. *Cancer Treat Rep.* 1987;71:267-272.

13. Yokote R, Tokura Y, Igarashi N, Ishikawa O, Miyachi Y. Photosensitive drug eruption induced by flutamide. *Eur J Dermatol.* 1998;8:427-429.

14. Lee K, Oda Y, Sakaguchi M, Yamamoto A, Nishigori C. Drug-induced photosensitivity to bicalutamide - case report and review of the literature. *Photodermatol Photoimmunol Photomed.* 2016;32:161-164.

15. Sortino S, Giuffrida S, De Guldi G, et al. The photochemistry of flutamide and its inclusion complex with beta-cyclodextrin. Dramatic effect of the microenvironment on the nature and on the efficiency of the photodegradation pathways. *Photochem Photobiol.* 2001;73:6-13.

16. Sasada K, Sakabe J, Tamura A, et al. Photosensitive drug eruption induced by bicalutamide within the UVB action spectrum. *Eur J Dermatol.* 2012;22:402-403.

17. Speers C, Zhao SG, Chandler B, et al. Androgen receptor as a mediator and biomarker of radioresistance in triple-negative breast cancer. *NPJ Breast Cancer.* 2017;3:29.

18. Zois CE, Koukourakis MI. Radiation-induced autophagy in normal and cancer cells: towards novel cytoprotection and radio-sensitization policies? *Autophagy.* 2009;5:442-450.

19. Schneider BP, Winer EP, Foulkes WD, et al. Triple-negative breast cancer: risk factors to potential targets. *Clin Cancer Res.* 2008;14:8010-8018.

20. Park S, Koo J, Park HS, et al. Expression of androgen receptors in primary breast cancer. *Ann Oncol.* 2010;21:488-492.

21. Gucalp A, Tolaney S, Isakoff SJ, et al. Phase II trial of bicalutamide in patients with androgen receptor-positive, estrogen receptor-negative metastatic Breast Cancer. *Clin Cancer Res.* 2013;19:5505-5512.

22. Labrie F, Bélanger A, Luu-The V, et al. Gonadotropin-releasing hormone agonists in the treatment of prostate cancer. *Endocr Rev.* 2005;26:361-379.

23. Goodwin JF, Schiewer MJ, Dean JL, et al. A hormone-DNA repair circuit governs the response to genotoxic insult. *Cancer Discov.* 2013;3:1254-1271.

24. Polkinghorn WR, Parker JS, Lee MX, et al. Androgen receptor signaling regulates DNA repair in prostate cancers. *Cancer Discov.* 2013;3:1245-1253.

25. Verheij M, Bartelink H. Radiation-induced apoptosis. *Cell and Tissue Research.* 2000;301:133-142.

26. He L, Kim SO, Kwon O, et al. ATM blocks tunicamycin-induced endoplasmic reticulum stress. *FEBS letters.* 2009;583:903-908.

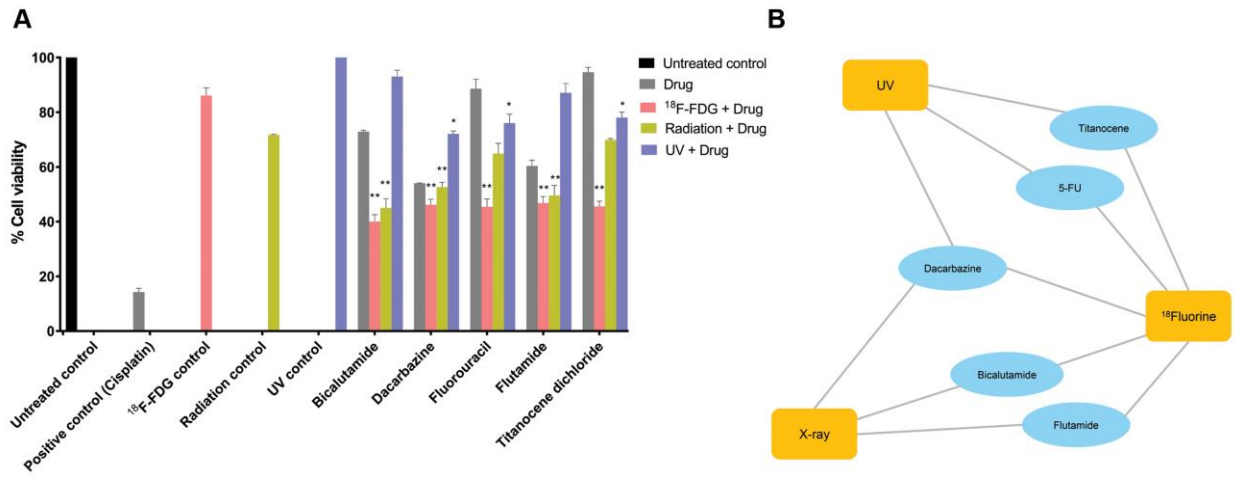

Figure 1. (A) Screening of FDA approved drugs in MDAMB231 cells and evaluation of cell toxicity in combination with ^{18}F-FDG, UV light and x-ray exposure. Data are statistically significant with *p<0.01 & **p<0.001. (B) Schematic representation of drugs classified based on response to ^{18}F-FDG, UV light, and x-rays.

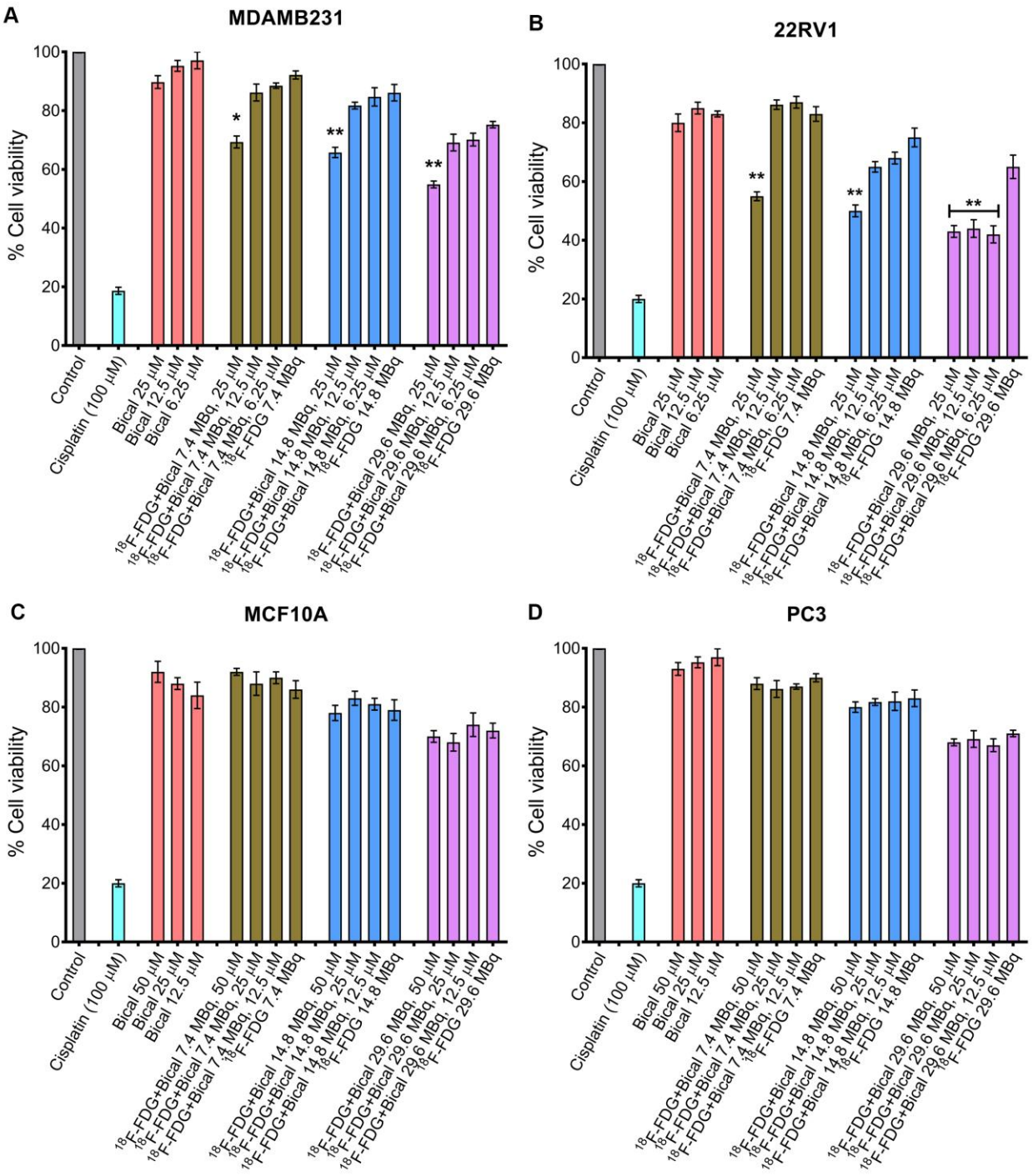

Figure 2. Cytotoxicity of Bical-^{18}F-FDG treatment for 72 hours, in (A) MDAMB231, (B) 22RV1, (C) MCF10A and (D) PC3cells. *p<0.01 & **p<0.001.

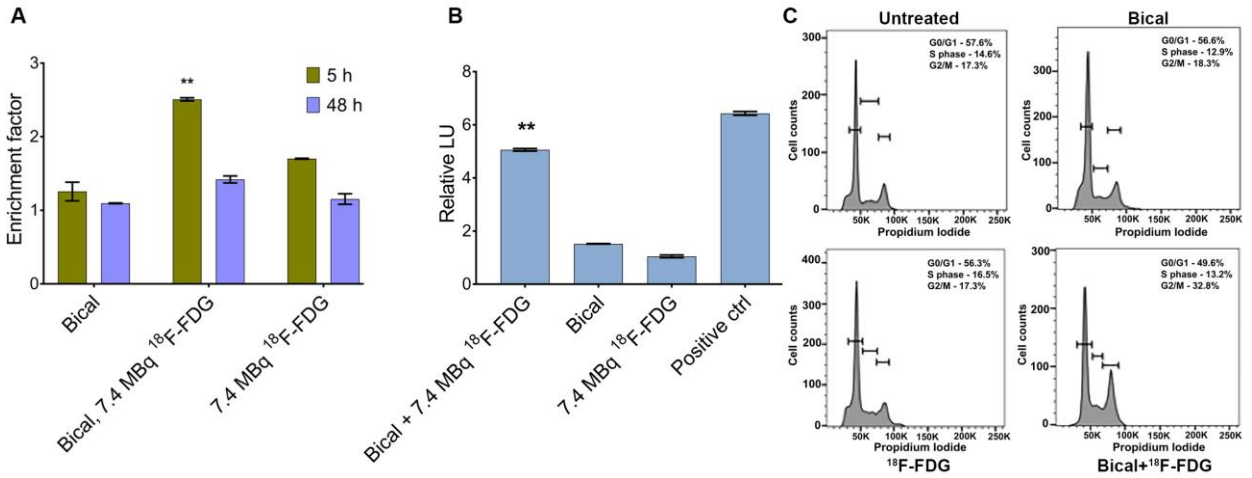

Figure 3. (A) Evaluation of DNA damage in Bical-^{18}F-FDG treated MDAMB231 cells by ELISA-based detection of mono- & oligonucleosomes (DNA fragments) as a result of DNA fragmentation (B) Luminescent measurement of phosphorylated γH2AX protein that occurred as a result of DNA damage within the cells (C) Determination of cell cycle arrest in various phases due to DNA damage in Bical-^{18}F-FDG treated cells. **$p<0.001$.

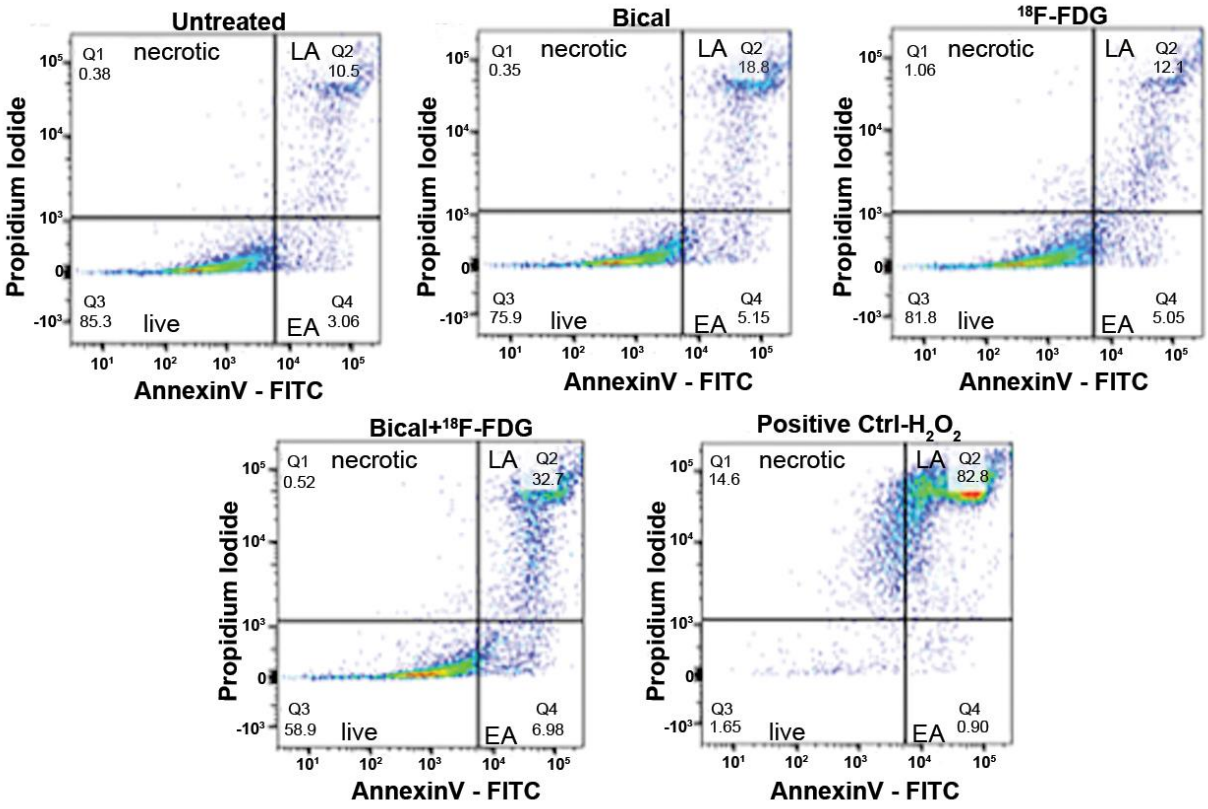

Figure 4. Flow cytometric quantification of Bical-^{18}F-FDG treated MDAMB231 cells undergoing apoptosis in various apoptotic stages.

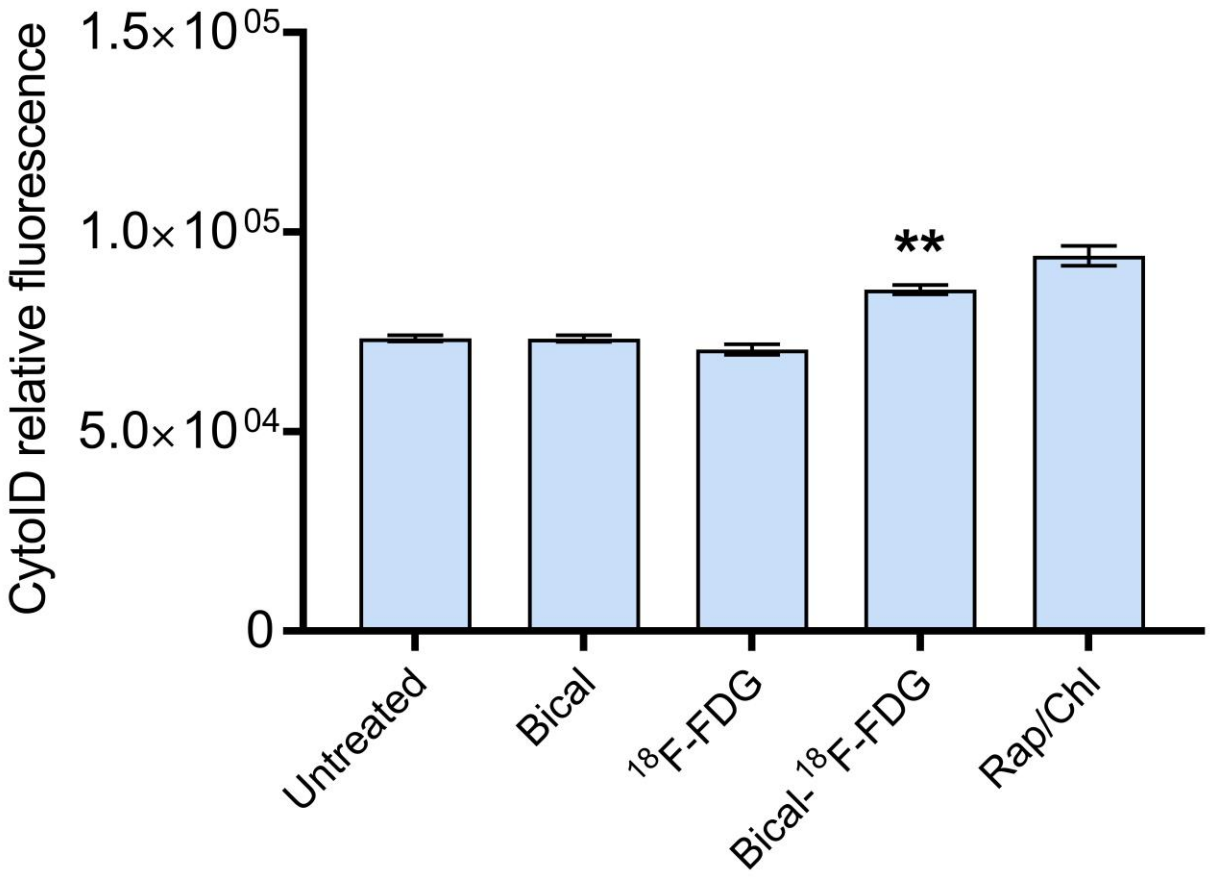

Figure 5. Flow cytometric quantification of Bical-^{18}F-FDG treated MDAMB231 cells undergoing autophagy. Rapamycin/Chloroquine treated cells used as a positive control. **p<0.001.

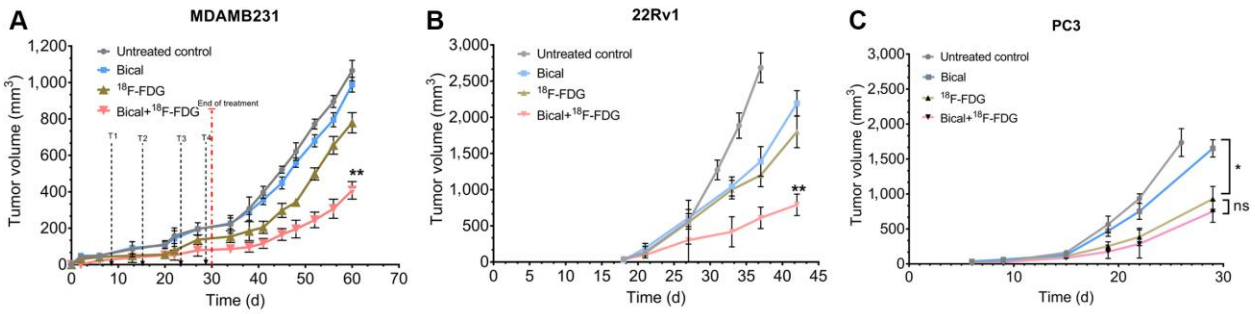

Figure 6. Tumor growth demonstrating therapeutic efficacy of combined treatment of Bical-^{18}F-FDG in a Athymic nude xenograft tumor model induced with subcutaneous (A) MDAMB231 cancer cells, (B) 22RV1 cancer cells, (C) PC3 cancer cells. N=5/group. *p<0.01 & **p<0.001.

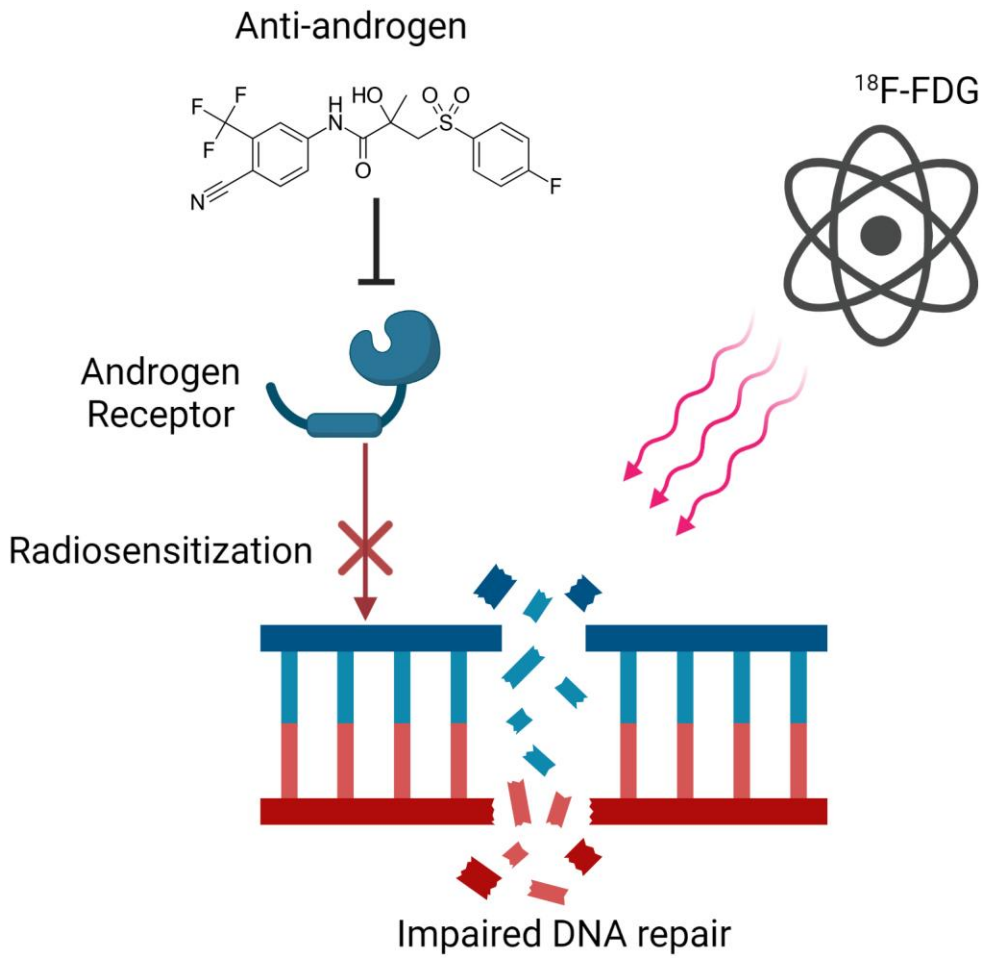

Graphical Abstract

Anti-Androgen Therapy Radiosensitizes Androgen Receptor Positive Cancers to F-18 Fluorodeoxyglucose

SUPLLEMENTARY DATA

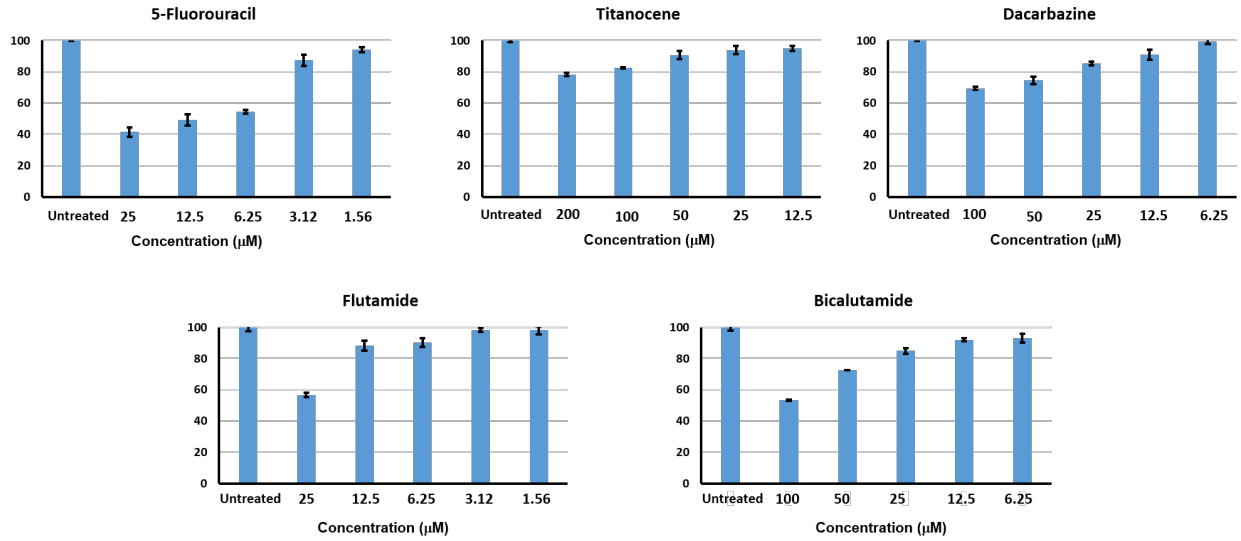

Supplemental Figure 1. Dark toxicity evaluation of 5-Fluorouracil, Titanocene, Dacarbazine, Flutamide and Bicalutamide in MDAMB231 cells. % viability of cells is measured using MTS assay after 72h incubation.

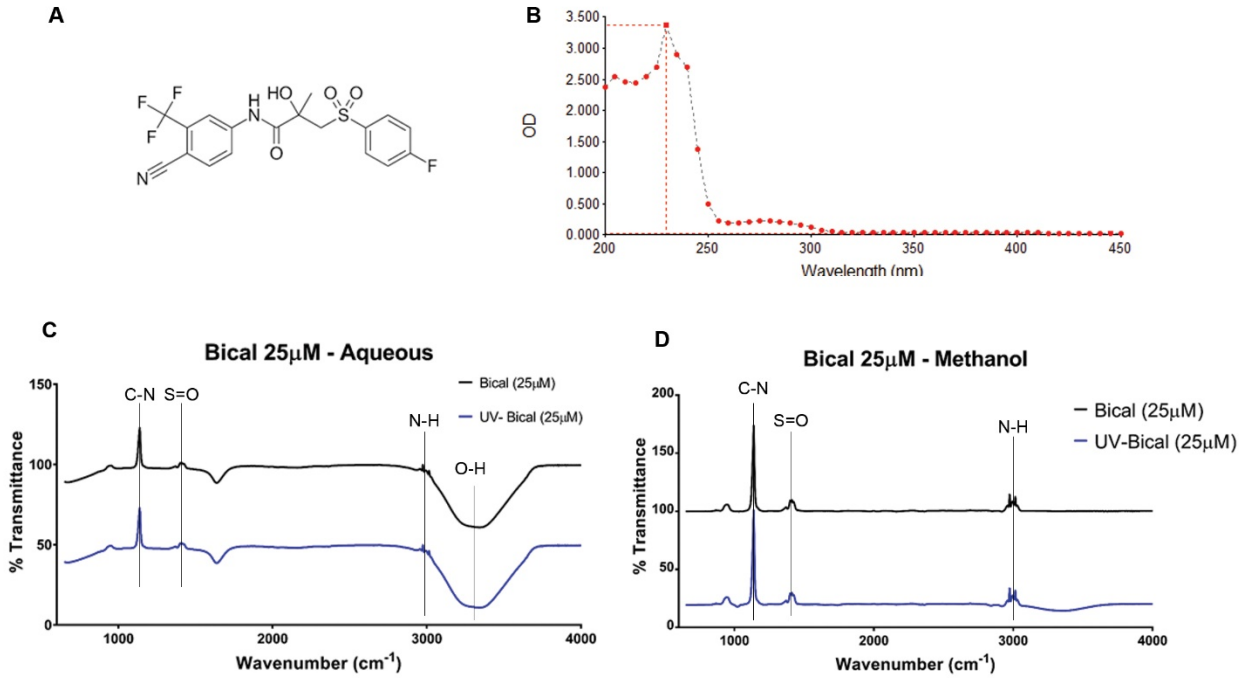

Supplemental Figure 2. (A) Chemical structure of Bicalutamide. (B) UV-vis absorption spectrum of Bicalutamide. (C) FTIR spectrum of Bical in aqueous phase showing no change in the functional groups with and without UV-radiation. (D) FTIR spectrum of Bical in methanol showing no change in the functional groups with and without UV-radiation.

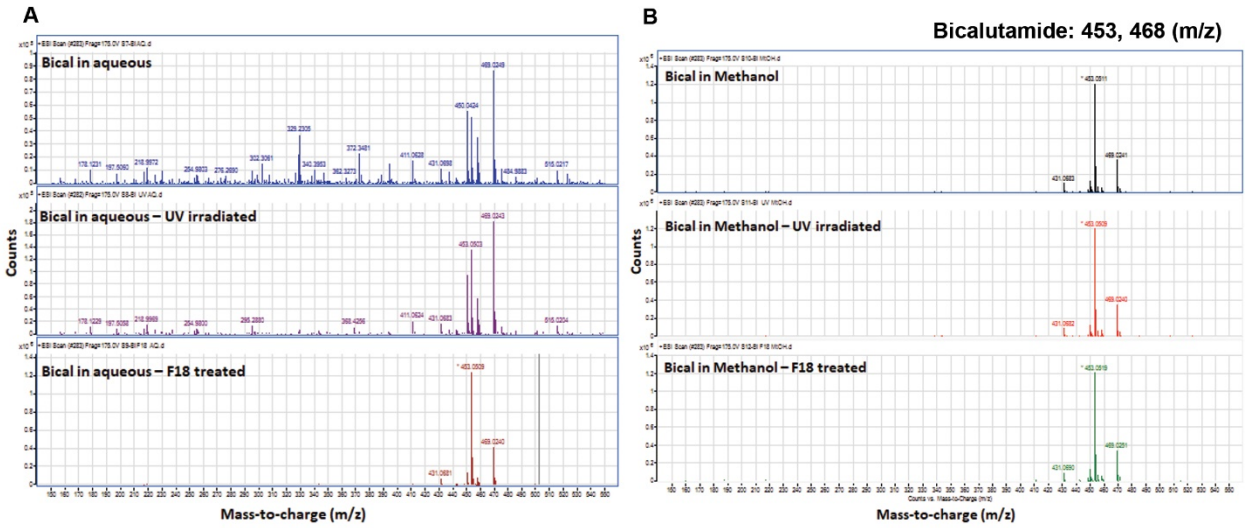

Supplemental Figure 3. (A) Mass spectrometry chromatogram of Bical in aqueous phase irradiated with UV and ^{18}F-FDG, showing no change in the molecular mass (453, 468 m/z). (B) Mass spectrometry chromatogram of Bical in methanol irradiated with UV and ^{18}F-FDG, also showing no change in the molecular mass (453, 468 m/z).

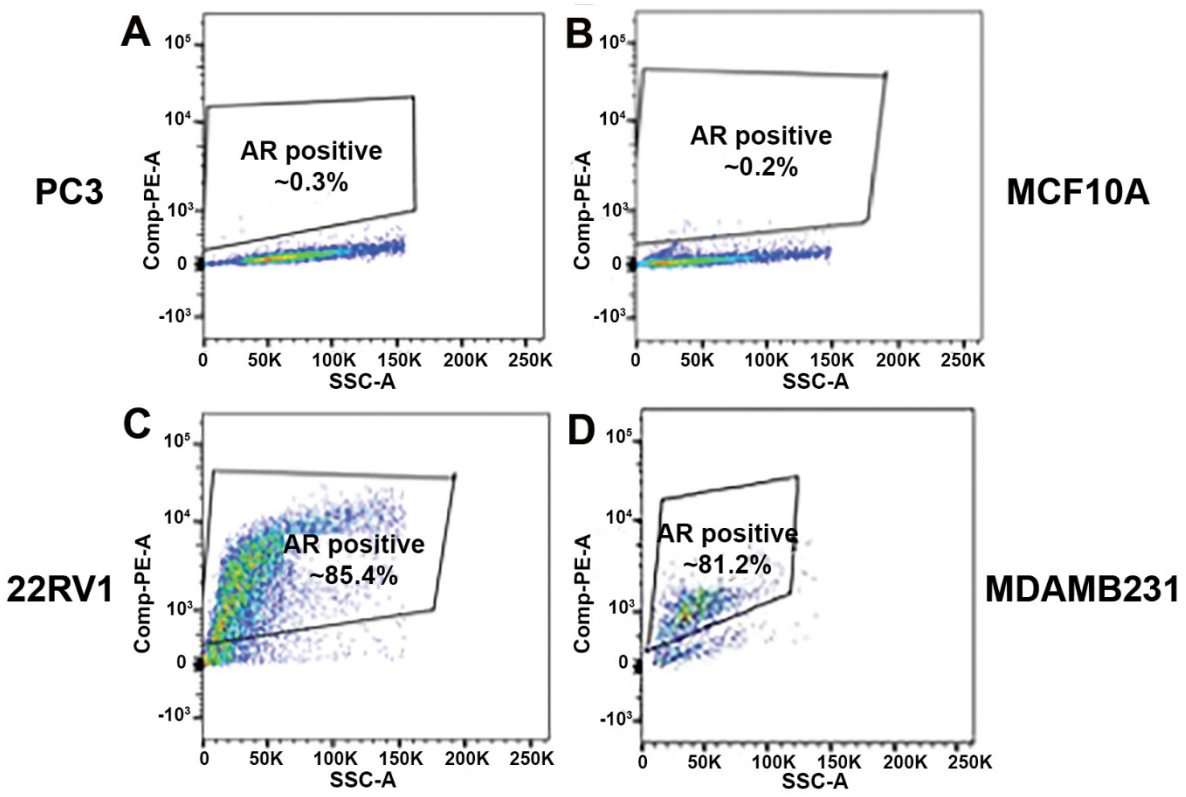

Supplemental Figure 4. Quantification of AR expression in (A) PC3 prostate cancer cells, (B) MCF10A normal breast epithelial cells, (C) 22RV1 prostate cancer cells and (D) MDAMB231 TNBC cells by Flow Cytometry.

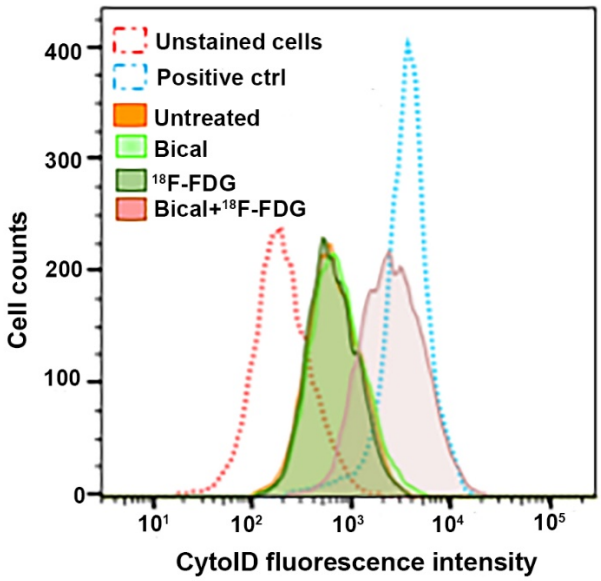

Supplemental Figure 5. Flow cytometer analysis of Bical-^{18}F-FDG treated MDAMB231 cells undergoing autophagy. Rapamycin/Chloroquine treated cells used as a positive control.

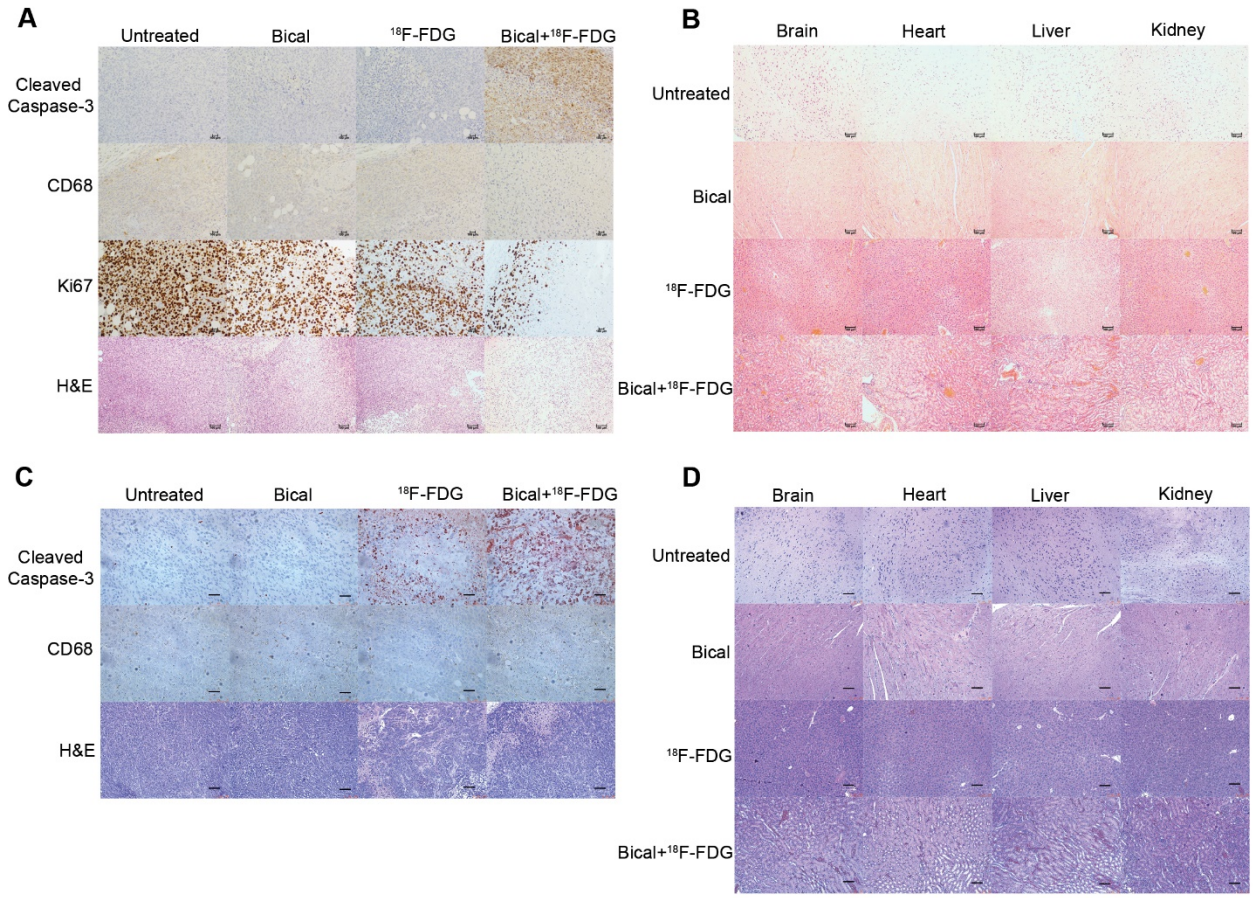

Supplemental Figure 6. (A) Immunohistochemical staining of xenograft MDAMB231 breast tumor tissues for expression of cleaved caspase-3, measuring tumor macrophage infiltration by CD68 positive staining and Ki67 expression quantification for high proliferating cancer cells, and H&E staining. (B) H&E staining of organs harvested from MDAMB231 tumor bearing mice to confirm the absence of cancer metastasis (Score: 0 for all organs) and minimal off-target toxicity to these vital organs. (C) Immunohistochemical staining of xenograft PC3 prostate tumor tissues for evaluating induction of apoptosis using a TUNEL assay, measuring tumor macrophage infiltration by CD68 positive staining and H&E staining. (D) H&E staining of organs harvested from PC3 tumor bearing mice to confirm the absence of cancer metastasis (Score: 0 for all organs) and minimal off-target toxicity to these vital organs. Scale bar is 100μm.

ADDITIONAL METHODS

Authentication of cell lines

The cells were authenticated for Mycoplasma presence using MycoAlert mycoplasma detection kit (Lonza). Cell lines were disregarded after 20 passages from thawing.

Drug screening in combination with ^{18}F-FDG

Cells were cultured in RPMI cell growth media supplemented with 10% Fetal bovine serum and 1% Pencillin-streptomycin at 37 °C under CO_2 atmosphere. For MTS assay cells were cultured in a 96 well plate at seeding density of 10,000 cells per well overnight. Cells were seeded in triplicates at three dilutions into 96-well plates and incubated for 12–16 hours prior to treatment.

Staining cells for flow cytometry

Cells were stained with fluorochrome conjugated primary antibody: PE conjugated AR (D6F11) XP® Rabbit monoclonal antibody (purchased from Cell Signaling Technology®). Cultured cells ($1\text{-}2x10^6$) were trypsinized and stained with Zombie UV dye for live/dead analysis. The stained cells were washed several times, fixed by 4% PFA and permeabilized by incubating the cells in 90% methanol at least for 30 minutes in ice. The fixed cells were stained with PE conjugated AR (volume ratio of 50:1) with final volume of 100µL 0.5% BSA.

Cell death detection assay

Cell death detection assay was carried out by the measurement of endo- and oligo-nucleosomes that are DNA fragments formed as a result of DNA damage which eventually leads to cell death due to apoptosis. Cells were harvested in 24 well plate with a seeding density $5x10^4$ per well,

with different groups of Bical-^{18}F-FDG along with control treatments of Bical, ^{18}FDG, and untreated cells in triplicate. Cells were washed and lysed at the end of the experiment. Cytoplasmic fractions of cell lysates were separated by centrifugation which contained the damaged DNA as a result of the treatments. Detection of DNA fragments was determined by an ELISA- based technique which involves binding of nucleosomes present in the cytoplasmic fraction via their histone components to the immobilized anti-histone antibody on the microwell plate [using Roche's Cell Death Detection kit]. It was then followed by addition of anti-DNA-peroxidase (POD) which reacts with the DNA-part of the nucleosome and washed thoroughly. The amount of peroxidase retained in the immunocomplex with ABTS (2, 2'-azino-di-[3-ethylbenzthiazoline sulfonate] substrate was determined by absorbance measurement at 405nm and 490nm (as reference wavelength). DNA damage was quantified by the measurement of mono- and oligo-nucleosomes, which is directly correlated with the enrichment factor measured. The enrichment factor was calculated by the ratio of the net absorbance (A_0) of treated cells to that of control cells in a Cytation I plate reader.

H2AX phosphorylation assay

Cells were fixed using 95% ethanol, 5% acetic acid and 1% formaldehyde, followed by treatment with a blocking buffer containing 3% BSA, for one hour at 37°C. Cells were then treated with primary antibody and incubated overnight at 4°C. After proper washing, cells were further treated with detection antibody and incubated for one hour at room temperature. The final step was to incubate the cells with the LumiGLO® chemiluminescent substrate solution and measure the luminescence between 10 and 20 minutes of incubation in a Cytation I plate reader.

Apoptosis, autophagy and cell cycle analysis

MDAMB231 cells were cultured in 6-well culture plates with a seeding density of $0.3x10^6$ and subjected to the treatments with Bical and ^{18}FDG. After 48 hours, the cells were washed properly in PBS and trypsinized with 0.25% Trysin-EDTA. The cells were washed thoroughly by centrifugation at 4°C and were stained with Biolegend's Annexin V-FITC and PI staining solution (1:2) prepared in Annexin V Binding buffer. After 15 minutes of incubation at RT in the dark, the samples were analyzed in a flow cytometer. Similarly, a set of cells samples after Bical-^{18}FDG treatment were collected after trypsinization and washed thoroughly in 1X assay buffer. After 30 minutes of incubation at 37°C in the dark, stained live cells were analyzed in a flow cytometer (BD/LSRII). For cell cycle analysis, MDAMB231 cells were cultured in 6-well plates with a density of 0.3 million cells per well. After 24 hours of post-treatment with Bical and ^{18}FDG, along with their controls, the cells were washed and fixed with 70% ethanol at 4°C for a minimum of one hour. The fixed cells were then stained with RNAse (0.1mg/mL) containing DNA staining PI red dye at the concentration of 20µg/mL at room temperature for 30 minutes. The stained cells were analyzed by flow cytometry for cell cycle arrest checkpoints in response to various treatments.

Animal studies

While 0.74 MBq dose of ^{18}F-FDG in mice is equivalent to a typical human PET scan, the basal metabolic rate per gram of body weight in mice is approximately seven times greater in mice than in humans, and the need for higher spatial resolution in mouse PET imaging necessitates using higher dose in mice for diagnostic imaging. Previous studies have demonstrated that a 0.74 MBq ^{18}F-FDG injection did not cause a significant increase in DNA

damage nor did it generate an adaptive response. The high injection activities such as 7.4 MBq, as used in this study, also did not lead to residual DNA damage as any damage caused was effectively repaired (*1*).

Tumor growth was measured every two days using Vernier calipers by using the formula: $(L \times W^2)/2$ (mm^3), where L is the longest axis and W the shortest axis. Animals were maintained in an Association for the Assessment and Accreditation of Laboratory Animal Care approved facility in accordance with current regulations of the U.S. Department of Agriculture and Department of Health and Human Services. Experimental methods were approved by and in accordance with institutional guidelines established by the Institutional Animal Care and Use Committee.

REFERENCES

1. Taylor K, Lemon JA, Boreham DR. Radiation-induced DNA damage and the relative biological effectiveness of 18F-FDG in wild-type mice. *Mutagenesis.* 2014;29:279-287.